2014 IEEE International Conference on Fuzzy Systems (FUZZ-IEEE)
July 6-11, 2014, Beijing, China

Adaptive unscented Kalman filter with a fuzzy supervisor for electrified drive train tractors

Pavel Osinenko, Mike Geissler, Thomas Herlitzius
Chair for Agricultural Systems and Technology
Technische Universität Dresden (TU Dresden), Dresden, Germany
Email: osinenko@ast.mw.tu-dresden.de

***Abstract*—Electrified drive trains for tractors are supposed to realize great potential of raising performance in heavy operations via optimal traction control. The paper proposes to apply an adaptive unscented Kalman filter (UKF) with a fuzzy supervisor for identification of electrical drive train tractor dynamics. The key advantage of electrical drive trains lies in feedback of drive torque which plays crucial role in traction parameter estimation. It is known that without using special adaptation techniques, an UKF may cause some divergence problems and lowered precision of estimation as well as its predecessor, an extended Kalman filter (EKF). A method based on a fuzzy logic supervisor in addition to adaptation of an UKF is proposed to maintain trade-off between tracking strength and estimation accuracy. Simulation results with a comprehensive tractor dynamics model showed increase in estimation precision of traction parameters. Laboratory experiments using a test stand with an electrical load machine showed appropriate estimation of the load torque**

***Index Terms*—Kalman filter, tire force, online identification, fuzzy logic, unscented transformation**

I. Introduction

One of the trends in development of agricultural machines and tractors is implementation of hybrid drive trains [1]. Among several advantages, like better drive train efficiency in comparison to conventional mechanical drives and lesser impact on the environment, they provide basis for continuous control of drive torques to enhance overall performance. A promising approach is an electrified drive train and, in particular, an electrified single-wheel drive [2]. Although electrical wheel-drives have yet some drawbacks in cost and mass of a vehicle, these disadvantages planned to be overcome in the nearest future by optimizing the construction of the drive. Thus, electrical drive trains have good prospects in cost-weight-comparison with mechanical and hydraulic ones and offer challenges in development of the concept of a “smart” drive train [3].

A. *Traction parameters and efficiency*

Traction efficiency and performance of farm tractors are characterized via several parameters which highly depend on slip [4] which is defined as follows:

$$
\begin{aligned}
s &= 1 - \tfrac{|v|}{r_d|\omega_w|} && \text{, if } |v| \le |r_d\omega_w|, \\
s &= -1 + \tfrac{r_d|\omega_w|}{|v|} && \text{, if } |v| > |r_d\omega_w|,
\end{aligned}
\tag{1}
$$

where v is the travelling velocity, r_d is the dynamic rolling radius and ω_w is the wheel revolution speed. The friction force coefficient μ is defined as follows (see [5], p. 319):

$$\mu = \frac{F_h}{F_z}, \tag{2}$$

where F_h is the horizontal force and F_z is the vertical load. The rolling resistance coefficient ρ consists of two parts: ρ_i – due to tire deformation and ρ_e – due to soil deformation:

$$\rho = \rho_e + \rho_i, \tag{3}$$

The net tractive ratio κ and the energy efficiency η_t are defined as follows:

$$\kappa = \mu - \rho_e, \tag{4}$$

$$\eta_t = \tfrac{\kappa}{\kappa+\rho}(1-s). \tag{5}$$

As can be seen on Fig. 1, soil conditions vary in a wide range yielding in general different maxima of energy efficiency.

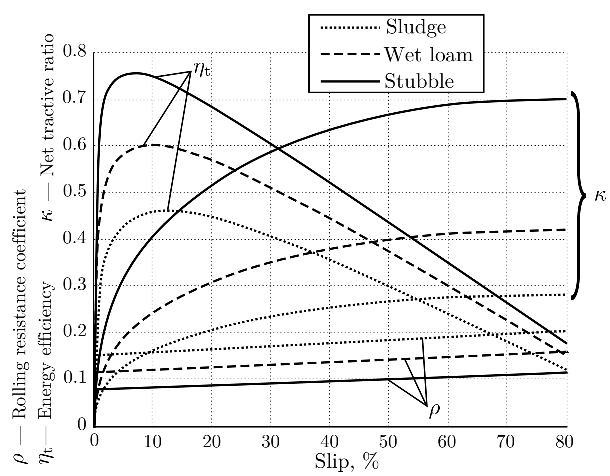

Fig. 1. Modeled traction characteristics for different soil types [2]

To define an optimal operating point (i.e. slip) with trade-off between efficiency and productivity, current traction parameter identification in real-time is necessary. These problems have been recently in the focus of research. Pichlmaier [6] addresses methods of determining drive torque and suggests to calculate the actual net tractive ratio and rolling resistance coefficient from these data together with draft force and wheel load measurement and use them to detect current soil conditions. This approach offers challenges in field of optimal usage of farm tractors, yet having certain drawbacks. As stated by Pichlmaier himself, identification of traction parameters is only possible if the velocity and wheel speed are constant, which is unlikely for farm tractors if taking into account measurement failures, irregularities of field micro- and macro-profile, draft force etc.. Current paper proposes a method for dynamic traction parameter estimation which can be further used for optimal traction control. To increase performance of identification, the design of a fuzzy inference system (namely, a fuzzy supervisor) for adaptation of an UKF is suggested.

B. Methods of tire-ground force identification

It is well known that measurement of forces acting from ground surface on a track or a tire is difficult and expensive. The same issue applies to measurement of the torque. On the other hand, there are many different approaches for identification of tire-ground contact dynamics. Eventually, they imply usage of one or another ground friction model. A substantial analysis of different static and dynamic tire-ground interaction models has been carried out (see for example [7], [8]). Some methods of online identification of the friction coefficient are based on adaptive techniques (see for example [9]). However, the difficulty of many classic adaptive algorithms based on finding a Lyapunov candidate function (LCF) lies in an assumption that unknown model parameters enter the model linearly which is a limitation for estimation of the friction coefficient. Ono et al. [10] uses an on-line least square method to estimate the extended braking stiffness (XBS) of the tire which enters the wheel deceleration model likewise linearly. Satisfactory results in estimation of both the longitudinal and lateral tire forces are obtained in [11] with use of filtering techniques for calculation of the friction coefficient derivative with respect to slip (i.e. XBS). Some authors use neural network estimators based on LuGre model of tire friction force [12]. On the other hand, a wide range of different filtering methods have shown appropriate results. Canudas-de-Wit et al. [13] proposes a non-linear observer to estimate the longitudinal tire-ground dynamics based on a lumped model. Kalman filter remains probably the most popular approach for identification of vehicle dynamics (see for example [14]–[16]). Taking into account the known computational difficulties of on-line tire-ground friction identification based on dynamic tire models, a static model is used in the present paper. The exact formula is a slightly changed variant from [5, p. 319]:

$$\mu = a_0 - c_0 e^{-b_0 s} - c_1 e^{-b_1 s}, \tag{6}$$

where a_0, c_0, c_1, b_0, b_1 are unknown parameters. Two exponents in (6) are supposed to capture different behavior in the low- and in the high-slip range.

C. Kalman filter approaches

A Kalman filter is in most cases the *de facto* approach for on-line system identification. An EKF which is typically used for non-linear identification problems may however undergo estimation precision deterioration and even divergence in case of high non-linearities in a system since it uses only first-order approximation (with a linearization term of Taylor series expansion) of system dynamics to propagate an estimate of mean and covariance of a Gaussian random variable (GRV). An UKF uses a set of sigma point to completely describe mean and covariance of a GRV and updates it through a non-linear state model yielding 2$^{\text{nd}}$order approximation of non-linearities [17] while having the same computational complexity order as EKF [18]. Besides some methods to address linearization problems (see for example [19]), an UKF does not require analytic computation of matrix Jacobians or Hessians at all. However, the main drawback stays the same for both types of Kalman filter and it lies in *a priori* knowledge of the state and measurement noise covariance which may cause flaws in state estimation and divergence [20]. Several approaches are successfully used to adapt Kalman filter to get better convergence in case of estimation failures by *increasing* the noise covariance. Many methods are based on noise statistic estimation. For example, a maximum likelihood approach is used in [21] to adjust the measurement and/or state noise covariance. Some experimental results with adaptation of the noise covariance are given in [22]. Soken et al. [23] applies multiple adaptation factors (or an adaptation matrix) in prediction of the estimate covariance which depends on the innovation vector. This approach is mainly applied to address sudden change in the noise covariance which result in significant increase of the residual between the predicted and the measured output, i.e. estimation failure. The factor is computed via covariance of the residual. A malfunction is detected via comparison of a statistical function (a quadratic form of the residual and the predicted measurement covariance having χ^2-distribution with the number of degrees of freedom equal to the dimensionality of the measurement vector) with the corresponding threshold. Although the proposed algorithm can successfully fix failures in estimation, it does not imply adaptation when the statistical criterion below the threshold, while the residual stays unsatisfactory for some purposes of vehicle longitudinal dynamics identification. There are also some methods to use a Kalman filter itself as a noise statistic estimator, this is so called "master-slave" filter. For example, Cui et al. [24] uses a combination of a particle filter and an UKF and proposes a method to reduce high computational complexity of the particle filter. An approach based on the MIT rule (named after the Massachusetts Institute of Technology) using partial derivatives of sigma points with respect to the state noise covariance diagonal elements is proposed in [25] to recursively solve an optimization problem in terms of the actual and computed innovation covariance. Nevertheless, for tractors, calculation of partial derivatives is of high computational complexity and might not fit the controller area network (CAN) with its relatively large sample times. Another approach of using an additional Kalman filter as a noise statistic estimator is suggested in [26]. However, the complexity of master-slave filters stays inappropriate for tractor microcontrollers. Many of noise statistic estimators are based on some optimization problem. A maximum *a posterior* (MAP) helps to update noise covariance by maximizing unconditional density function of estimate [27]. There are also ways to adapt Sage-Husa estimators usually used for an EKF to work with an UKF [28]. The designed algorithm adjusts the state and measurement noise covariance with a certain fading factor. A similar procedure is suggested in [29], but with use of a moving window method. Such methods are also used for adaptation of either Kalman matrix or the prior estimate covariance which comprises a fading factor calculated via a windowed innovation covariance. A fused estimation from multiple Kalman filters based on adaptive fading helps to improve identification in case of asynchronous measurement [30]. On the other hand, application of fuzzy logic for Kalman filters also demonstrated success in detecting divergence and estimating of the state and measurement noise covariance. For example, Abdelnour et al. [31] uses a fuzzy logic supervisor (FLS) to adjust a scaling factor in the exponential weighting scheme for the estimate covariance. The mean and covariance of the innovation are used to detect divergence and a FSL is turned on when they fail testing for white noise. An approach using a so called degree of matching (DoM) between theoretical innovation covariance and its estimated value (via windowed estimation) is suggested for detecting estimation failures and increasing/decreasing either the state or measurement noise covariance in [32]. This algorithm implies purely fuzzy logical adjustment of the noise covariance. Somewhat similar method, but with help of a neural network, is proposed in [33], this is a so called adaptive neuro-fuzzy extended Kalman filter (ANFEKF). Apart from these approaches, a new fuzzy supervisor works together with a conventional adaptation algorithm. A combination of fuzzy systems with conventional adaptation algorithms for Kalman Filter can be met in literature as well (see for example [34]). Here, a so called fuzzy logic adaptation system (FLAS) is used to additionally adjust tuning parameters of a suboptimal scaling matrix for adaptation of the state covariance of a strong tracking unscented Kalman filter (STUKF) via a so called degree of divergence (DoD) and the averaged magnitude of the innovation. The methodology of the present work involves besides the innovation vector the measurement itself to adjust the noise covariance in case if the filter operates normally. Usage of the measurement to adapt a Kalman filter can be met in [35] where a fuzzy logic system produces a fuzzy-adaptive parameter for the estimate covariance depending of which state the system is.

II. Methodology

A. Short description of an UKF

Consider a non-linear model of a system in the following discrete form:

$$\begin{aligned} x_k &= f\left(x_{k-1}, u_{k-1}\right) + q_{k-1}, \\ y_k &= h(x_k) + r_k, \end{aligned} \tag{7}$$

where $x_k \in \mathbb{R}^n$ is the state vector, $u_k \in \mathbb{R}^p$ is the input vector, $y_k \in \mathbb{R}^m$ is the output vector, $f\left(x_{k-1}, u_{k-1}\right)$ is the non-linear state model, $h(x_k)$ is the measurement model, $q_k \sim \mathcal{N}(0, \mathbf{Q}_k), r_k \sim \mathcal{N}(0, \mathbf{R}_k)$ are the state and measurement noises with zero mean and covariance $\mathbf{Q}_k, \mathbf{R}_k$ respectively, k is the time step counter. The main difference between an UKF and an EKF lies in calculation and propagation of so called sigma-points instead of linearization of the state and measurement models in (7) via an unscented transform (UT). Given a mean and covariance, a properly chosen set of sigma-points is computed having, therefore, a discrete probability distribution with second central moments completely matching to ones of the underlying probability distribution, whatever it was [36]. The algorithm of identification of the state vector in (7) with an UKF consists of the following steps [18]:

- **Initialization**
  For some initial guess x_0, set the mean and covariance as follows:
  $\hat{x}_0 = \mathbb{E}\left[x_0\right],$
  $\mathbf{P}_0 = \mathbb{E}\left[(x_0 - \hat{x}_0)(x_0 - \hat{x}_0)^T\right]$, where $\mathbb{E}\left[\bullet\right]$ denotes the expectation value operator.
- **Prediction** (for steps $k = 1 ... \infty$)
  Compute $2n+1$ sigma-points of the state as follows:
  $\chi_{k-1}^{(0)} = \hat{x}_{k-1},$
  $\chi_{k-1}^{(i)} = \hat{x}_{k-1} + \sqrt{n+\lambda}\left(\sqrt{\mathbf{P}_{k-1}}\right)_i,$
  $\chi_{k-1}^{(n+i)} = \hat{x}_{k-1} - \sqrt{n+\lambda}\left(\sqrt{\mathbf{P}_{k-1}}\right)_i, i = 1...n,$
  where $(\bullet)_i$ denotes the i^{th}column of a matrix and $\sqrt{\mathbf{P}}$ denotes matrix square root of a matrix $\mathbf{P}$ satisfying:
  $\sqrt{\mathbf{P}}\left(\sqrt{\mathbf{P}}\right)^T = \mathbf{P}$ and calculated via Cholesky decomposition; $\lambda = \alpha^2(n+\kappa) - n$ is a scaling parameter with α and κ characterizing the spread of sigma points around mean (chosen as tuning parameters).
  Compute weights of the sigma-points:
  $\mathcal{W}_m^{(0)} = \dfrac{\lambda}{n+\lambda},$
  $\mathcal{W}_c^{(0)} = \dfrac{\lambda}{n+\lambda} + \left(1 - \alpha^2 + \beta\right),$
  $\mathcal{W}_m^{(i)} = \dfrac{\lambda}{2(n+\lambda)},$
  $\mathcal{W}_c^{(i)} = \dfrac{\lambda}{2(n+\lambda)}, i = 1...2n$
  with an additional parameter β which allows to incorporate any *a priori* knowledge of the probability distribution of the state.
  Perform time update of the sigma-points using the model (7):
  $\chi_{k|k-1}^{(i)} = f(\chi_{k-1}^{(i)}, u_{k-1}).$
  Compute the predicted estimate mean and covariance:
  $\hat{x}_{k|k-1} = \sum_{i=0}^{2n} \mathcal{W}_m^{(i)} \chi_{k|k-1}^{(i)},$
  $\mathbf{P}_{k|k-1} = \sum_{i=0}^{2n} \mathcal{W}_c^{(i)}\left(\chi_{k|k-1}^{(i)} - \hat{x}_{k|k-1}\right) \cdot$
  $\left(\chi_{k|k-1}^{(i)} - \hat{x}_{k|k-1}\right)^T + \mathbf{Q}_{k-1}.$

- **Measurement update**
  Compute $2n+1$ sigma-points of the state as follows:
  $\chi_{k|k-1}^{(0)} = \hat{x}_{k|k-1}$,
  $\chi_{k|k-1}^{(i)} = \hat{x}_{k|k-1} + \sqrt{n+\lambda}\left(\sqrt{\mathbf{P}_{k|k-1}}\right)_i$,
  $\chi_{k|k-1}^{(n+i)} = \hat{x}_{k|k-1} - \sqrt{n+\lambda}\left(\sqrt{\mathbf{P}_{k|k-1}}\right)_i, i = 1...n$.
  Perform measurement update of the sigma points:
  $\Upsilon_k^{(i)} = h(\chi_{k|k-1}^{(i)})$.
  Compute the predicted output mean and innovation covariance:
  $\hat{y}_k = \sum_{i=0}^{2n} \mathcal{W}_m^{(i)} \Upsilon_k^{(i)}$,
  $\mathbf{S}_k = \sum_{i=0}^{2n} \mathcal{W}_c^{(i)} \left(\Upsilon_k^{(i)} - \hat{y}_k\right)\left(\Upsilon_k^{(i)} - \hat{y}_k\right)^T + \mathbf{R}_k$.
  Compute the cross-covariance of the state and measurement:
  $\mathbf{C}_k = \sum_{i=0}^{2n} \mathcal{W}_c^{(i)} \left(\chi_{k|k-1}^{(i)} - \hat{x}_{k|k-1}\right)\left(\Upsilon_k^{(i)} - \hat{y}_k\right)^T$.
  Compute the filter gain, conditional estimated mean and covariance given the actual measurement y_k:
  $\mathbf{K}_k = \mathbf{C}_k \mathbf{S}_k^{-1}$,
  $\hat{x}_k = \hat{x}_{k|k-1} + \mathbf{K}_k\left(y_k - \hat{y}_k\right)$,
  $\mathbf{P}_k = \mathbf{P}_{k|k-1} - \mathbf{K}_k \mathbf{S}_k \mathbf{K}_k^T$.

B. Model of tractor longitudinal dynamics

Translational dynamics of the tractor is described as follows:

$$m\dot{v} = \sum_{\alpha=1}^{N} F_{h,\alpha} - F_d - F_{rr,e}. \tag{8}$$

where m is the tractor mass, F_d is the draft force, i.e. resistance of the implement, $F_{rr,e} = \rho_e F_g$ is the rolling resistance force due to soil deformation (or external rolling resistance), F_g is the vehicle weight and α denotes the wheel index. The horizontal force is computed via (6). The dynamics of the wheel reads as follows:

$$\dot{\omega}_w = \tfrac{1}{J_w}\left(M_d - r_d F_z\left(\mu + \rho_i\right)\right), \tag{9}$$

where J_w is the wheel inertia, M_d is the drive torque. The wheel load torque is: $M_l = r_d F_z\left(\mu + \rho_i\right)$. For an electrified drive train, the wheel drive torque is defined with the following model:

$$\begin{aligned} \dot{M}_e &= -\tfrac{1}{\tau_e}\left(M_e - M_{\text{con}}\right), \\ M_d &= i_g M_e, \end{aligned} \tag{10}$$

where M_e is the electrical motor torque, $M_{con} = u$ is the control input, τ_e is the electrical time constant, i_g is the gear ratio from the electrical motor to the wheel. The tire dynamic rolling radius is: $r_d = r_0 - \triangle f$ with r_0 being the unloaded tire radius and $\triangle f$ is the tire radial deformation which can be estimated using a linear empirical formula given in [37, p. 40]:

$$\triangle f = \frac{F_z}{2\pi \cdot 10^5 \cdot p_t \sqrt{r_0 b_t / 2}},$$

where p_t is the tire air pressure in [bar] and b_t is the tire section width. The draft force is usually measured. The wheel loads are supposed to be either measured (by hydraulic pressure sensors of suspension) or estimated (see for example [38]). The inner rolling resistance coefficient on a loose soil ρ_i can be approximated from that on a rigid surface, which is known for a specific tire [39]. Equations (6) and (9) must be used for every single wheel indexed by $\alpha = 1...N$. Identification is performed in terms of an unknown parameter vector which is formulated as follows:

$$\begin{aligned} \theta_\alpha &= \left(a_{0,k}, c_{0,\alpha}, b_{0,\alpha}, c_{1,\alpha}, b_{1,\alpha}\right)^T, \alpha = 1...N \\ \theta &= \left(\theta_1, \theta_2, ..., \theta_N, \rho_e\right)^T. \end{aligned} \tag{11}$$

Therefore, the following augmented state vector is considered:

$$x = \begin{pmatrix} M_{e,1}, ..., M_{e,N}, & \omega_{w,1}, ..., \omega_{w,N}, & v, & \theta^T \end{pmatrix}^T. \tag{12}$$

The measurement vector is defined as follows:

$$y = \begin{pmatrix} \omega_{w,1}, \omega_{w,2}, ..., \omega_{w,N}, & v \end{pmatrix}^T. \tag{13}$$

The input vector reads as:

$$u = \begin{pmatrix} M_{\text{con},1}, M_{\text{con},2}, ..., M_{\text{con},N} \end{pmatrix}^T. \tag{14}$$

The auxiliary signals $F_{z,1}, ..., F_{z,N}$, $r_{d,1}, ..., r_{d,N}$, $\rho_{i,1}, ..., \rho_{i,N}$, F_d are used additionally in the state model, but computed (or measured) outside. Propagation of the sigma points through the model is maintained using the fourth-order Runge–Kutta method. Dynamics of the unknown parameter vector (11) is modeled using the following equations:

$$\theta_k = \theta_{k-1}, \tag{15}$$

assuming that parameters change slowly in time. Hence, (11) is estimated using a random-walk procedure in terms of Kalman filter approach. The net tractive ratio κ is computed in terms of the whole vehicle as well as the external rolling resistance coefficient ρ_e and reads as:

$$\begin{aligned} \kappa = & \frac{\sum_{\alpha=1}^{N}\left(a_{0,\alpha} - c_{0,\alpha}e^{-b_{0,\alpha}s_\alpha} - c_{1,\alpha}e^{-b_{1,\alpha}s_\alpha}\right)F_{z,\alpha}}{F_g} - \\ & - \rho_e, \alpha = 1...N. \end{aligned} \tag{16}$$

C. Adaptation mechanism of an UKF

In case if the noise covariance is *a priori* unknown, changes with time or in case of measurement fault, it is necessary to adapt the filter. While the measurement noise covariance can be set up using extensive knowledge of specific sensor accuracy for agricultural machinery, the state noise covariance stays in most cases unknown. Recall firstly the definition of the theoretical innovation covariance given in II-A in order to build the adaptation mechanism:

$$\mathbf{S}_k = \sum_{i=0}^{2n} \mathcal{W}_c^{(i)} \left(\Upsilon_k^{(i)} - \hat{y}_k \right) \left(\Upsilon_k^{(i)} - \hat{y}_k \right)^T + \mathbf{R}_k. \tag{17}$$

When the filter works normally, the innovation sequence appears to be a zero-mean Gaussian white noise and with the covariance (17) matching the actual innovation covariance. The second one can be estimated with use of a forgetting factor (see for example [34]) or simply via windowed estimation:

$$\bar{\mathbf{S}}_k = \frac{1}{M-1} \sum_{i=k-M+1}^{k} \left(y_k - \hat{y}_k \right) \left(y_k - \hat{y}_k \right)^T. \tag{18}$$

where M is the moving window size which is chosen to be greater than the number of states n in order to avoid destabilization of the filter according to [21]. For criteria of choosing an appropriate window size one can refer to [40]. Notice that all terms in the window contribute equally which is different to the usage of a forgetting factor. (18) helps to gather the necessary statistical information about the innovation sequence online. Further, the theoretical innovation covariance (17) must equal to the actual one (18):

$$\mathbf{S}_k = \bar{\mathbf{S}}_k. \tag{19}$$

As was mentioned above, the main difficulty of identification is in knowledge of the state noise covariance. In this sense, it is suggested to adjust the state noise covariance instead of the measurement noise covariance. In order to achieve this, recall the definition of an UKF. Using the definition of the Kalman gain from II-A for (19) yields:

$$\begin{aligned} K_k \mathbf{S}_k K_k^T = K_k \bar{\mathbf{S}}_k K_k^T \iff \\ \mathbf{P}_{k|k-1} - \mathbf{P}_k = K_k \bar{\mathbf{S}}_k K_k^T \iff \\ \sum_{i=0}^{2n} \mathcal{W}_c^{(i)} \left(\chi_{k|k-1}^{(i)} - \hat{x}_{k|k-1} \right) \cdot \\ \left(\chi_{k|k-1}^{(i)} - \hat{x}_{k|k-1} \right)^T + \mathbf{Q}_{k-1} - \mathbf{P}_k = K_k \bar{\mathbf{S}}_k K_k^T. \end{aligned} \tag{20}$$

In order to adapt the filter, the predicted estimate covariance must be modified to satisfy (20). As can be seen, there are several methods to introduce an adaptation factor to the aforementioned equation, in particular it can be done via scaling the whole predicted estimate covariance or the Kalman gain directly (see for example [30]). In general, an adaptive scaling does not have to be scalar. As was stated in [23] for high-order systems, the filter performance is different for different states in (12), thus usage of multiple adaptive factors (an adaptive matrix) can be applied in more effective way than a single adaptive factor. Using this fact, modify (20) as follows:

$$\begin{aligned} \sum_{i=0}^{2n} \mathcal{W}_c^{(i)} \left(\chi_{k|k-1}^{(i)} - \hat{x}_{k|k-1} \right) \cdot \\ \left(\chi_{k|k-1}^{(i)} - \hat{x}_{k|k-1} \right)^T + \mathbf{A}_k \mathbf{Q}_{k-1} - \mathbf{P}_k = K_k \bar{\mathbf{S}}_k K_k^T, \end{aligned} \tag{21}$$

where $\mathbf{A}_k$ is an adaptive matrix needed to additionally adjust the state noise covariance so that (19) is fulfilled.

Lemma 1: Adaptive scaling matrix for an UKF

Supposing there is a positive real number $q_{\text{min}} > 0$ such that $q_{\text{min}} \mathbf{I}_n \leq \mathbf{Q}_k$ for $k = 0, 1, 2...$, where $\mathbf{I}_n$ denotes an $n \times n$ unit matrix, then the suboptimal adaptive matrix for (21) is computed as:

$$\begin{aligned} \mathbf{A}_k = \Bigg(K_k \bar{\mathbf{S}}_k K_k^T - \sum_{i=0}^{2n} \mathcal{W}_c^{(i)} \left(\chi_{k|k-1}^{(i)} - \hat{x}_{k|k-1} \right) \cdot \\ \left(\chi_{k|k-1}^{(i)} - \hat{x}_{k|k-1} \right)^T + \mathbf{P}_k \Bigg) \mathbf{Q}_{k-1}^{-1}, \end{aligned} \tag{22}$$

Proof: Follows from positive definiteness of $\mathbf{Q}_{k-1}$.

Remark 2: The condition of the lemma states that if the measurement noise covariance is positive-definite for all steps $k = 0, 1, 2...$ (in particular, if it is set up at its initial guess which is positive-definite and stays unchanged) then the suboptimal adaptive matrix is well-defined.

Thus, the updated estimate covariance is modified in the following way:

$$\begin{aligned} \mathbf{P}_k = \sum_{i=0}^{2n} \mathcal{W}_c^{(i)} \left(\chi_{k|k-1}^{(i)} - \hat{x}_{k|k-1} \right) \cdot \\ \left(\chi_{k|k-1}^{(i)} - \hat{x}_{k|k-1} \right)^T + \mathbf{A}_k \mathbf{Q}_{k-1} - K_k \mathbf{S}_k K_k^T. \end{aligned} \tag{23}$$

Due to computational issues, the adaptive matrix may appear not to be diagonal. On the other hand, when its diagonal elements are lesser than 1, the filter is supposed to be in a stable state. Hence, the elements of the adaptive matrix are modified as follows:

$$\mathbf{A}_k = \{a_{ij}\}_{\substack{i=1 \\ j=1}}^{n} = \begin{cases} \min\{1, a_{ij}\} & , i = j \\ 0 & , i \neq j. \end{cases} \tag{24}$$

In case of an estimation fault, if the filter fails to converge, the adaptation mechanism introduces a scaling matrix to the state noise covariance by increasing it in a certain way. It can be seen that if $\mathbf{A}_k = \mathbf{I}_n$, the adaptive filter coincides with an ordinary UKF given in II-A. Given the adaptation mechanism (18), (22), (23) an adaptive UKF (or AUKF) is built. An AUKF helps to address convergence issues of an ordinary UKF by adjusting the state noise covariance for each state individually.

D. Fuzzy supervisor for the AUKF

The adaptation mechanism is "switched on" increases diagonal elements of (24) in case of an estimation failure. For practical goals related to agricultural machinery, it is necessary, however, to additionally adjust the state noise covariance even in absence of an estimation failure. According to [34], when $a_{ij} \leq 1$, the filter operates in a stable mode. Given (15), an AUKF (which now coincides with an ordinary UKF) predicts the unknown parameters via a random-walk with "amount of step" characterized by the state noise covariance. On the other hand, greater elements of $\mathbf{Q}$ result in stronger tracking, while smaller values give less noisy estimation (or "smoothen" the estimate [22]). By inspection, increase of the state noise covariance, the updated estimate covariance $\mathbf{P}_k$ and, thus, the filter gain $\mathbf{K}_k$ yields better ability to follow the true mean. On the other hand, too large $\mathbf{Q}$ will make the filter overreact and produce non-smooth estimate. In general, it is recommended to keep $\mathbf{Q}$ as large as possible to avoid divergence (when the filter fails to react to strong change in system state) and keep satisfactory accuracy. As can be seen from (24), the AUKF does not imply decreasing the state noise covariance. Thus, the estimate may be too noisy, which is not recommended for use by tractor microcontrollers, even if the estimation is in stable mode. In order to achieve trade-off between filter's ability to overcome measurement failures and keep convergence on one side and estimation accuracy and smoothness on the other, a so called fuzzy supervisor (FS) is proposed to co-operate with the adaptation mechanism. Unlike the most of the fuzzy logic techniques applied to a Kalman filter, the FS is based on the measurement itself instead of the innovation. It is assumed that the innovation sequence is only used by the adaptation mechanism to detect estimation failure and eliminate it, while the FS is supposed to additionally adjust $\mathbf{Q}$ according to the needs of a traction control system (TCS). For tractors, a large change in system dynamics is related strong fluctuations of the draft force or field micro-profile followed by fluctuations of the wheel load torque and vehicle travelling velocity. Such effects can be generally captured by measurement of the wheel revolution speed and travelling velocity. Further, it can be concluded that the filter should track the state stronger during the aforementioned phases of large change in dynamics. Otherwise, $\mathbf{Q}$ may be decreased when the change is negligible and the tractor moves evenly. The main purpose of the FS is to adjust $\mathbf{Q}$ additionally in the stable phase using extra parameter for the adaptive matrix in the following way:

$$\mathbf{A}_k = \{a_{ij}\}_{\substack{i=1 \\ j=1}}^{n} = \begin{cases} \min\{\kappa_{\text{fuzz}}, a_{ij}\} & , i = j, a_{ij} \geq \kappa_{\text{fuzz}} \\ 0 & , i \neq j, \end{cases} \tag{25}$$

where $\kappa_{\text{fuzz}}, \bar{\kappa}_{\text{fuzz}} \leq \kappa_{\text{fuzz}} \leq 1$ is the fuzzy adjustment parameter and a real number $\bar{\kappa}_{\text{fuzz}} > 0$ is a tuning parameter indicating the lower bound of κ_{fuzz} and is fixed in the FS. The reason of the fuzzy adjustment parameter introduced such way is that it does not affect the ability of the adaptation mechanism to eliminate divergence via increasing $\mathbf{Q}$. Indeed, if the left-hand side of (21) becomes lesser than the right-hand side, the certain adaptive gains will take values $a_{ij} \geq \kappa_{\text{fuzz}} \geq 1$ which is consistent with the ordinary adaptation mechanism. The way to determine κ_{fuzz} is done via a Takagi-Sugeno (T-S) fuzzy system taking the measurement vector as its input. The FS captures amount of change in vehicle dynamics using the following difference equations for some step k:

$$\begin{aligned} \triangle\omega_w &= \left| \sum_{\alpha=1}^{N} \left(\omega_{w,\alpha}(k) - \omega_{w,\alpha}(k-L+1)\right) \right|, \\ \triangle v &= |v(k) - v(k-L+1)|, \end{aligned} \tag{26}$$

where L is the moving window size of the FS which helps to avoid measurement noise by taking two values located at appropriate distance. For simplicity, averaging is performed over all wheels indexed by $\alpha = 1...N$. Variables (26) are quantified using an empirical value $a_{\max}$ characterized by typical range of farm tractor acceleration (or approximately calculated given the vehicle mass and static axle weight distribution with an assumption of having a high friction force coefficient about $0.7 \div 0.8$, for concrete methods one can refer to [8]). Thus, quantification of the input is computed as follows:

$$q_\omega = \frac{\triangle\omega_w r_0}{a_{\max} L t_s}, q_v \quad = \frac{\triangle v}{a_{\max} L t_s}, \tag{27}$$

where t_s is the sample time and the corresponding fuzzy variables are W and V - amount of change in the wheel revolution speed and in the velocity respectively. The quantifiers can not be greater than 1: $q_\omega = \max\{1, q_\omega\}, q_v = \max\{1, q_v\}$. The fuzzy output variable is denoted Ψ. Three fuzzy levels are chosen to describe the fuzzy variables: Hi- "high", Av- "average" and Lo- "low". The corresponding bell-shaped membership functions are defined as follows:

$$\sigma_j(q_i) = \frac{1}{1 + \left| {}^{q_i - \lambda_j}/_{\xi} \right|^{2\zeta}},$$

where constants ζ and ξ characterize the spread and λ_j characterize the middle value of a curve, index i takes values of $\{\omega, v\}$ and index j takes values of $\{Hi, Av, Lo\}$. A fuzzy decision is made using the following rule base:

$$\begin{aligned} &(\text{if } V_{Lo} \text{ and } \neg W_{Hi}) \text{ or } (W_{Lo} \text{ and } \neg V_{Hi}) \text{ then } \Psi_{Lo} \\ &(\text{if } V_{Hi} \text{ and } \neg W_{Lo}) \text{ or } (W_{Hi} \text{ and } \neg V_{Lo}) \text{ then } \Psi_{Hi} \\ &\text{else } \Psi_{Av} \end{aligned} \tag{28}$$

with corresponding membership functions $\mathcal{R}_j, j \in \{Hi, Av, Lo\}$. Defuzzification is made via the discrete center of area (CoA) rule:

$$q_{\kappa,j} = \frac{\sum_{l=1}^{L} \left(\triangle q\cdot(l+1)\cdot\overline{\sigma}_j(\triangle q\cdot(l+1)) + \triangle q\cdot l\cdot\overline{\sigma}_j(\triangle q\cdot l)\right)}{\sum_{l=1}^{L} \left(\overline{\sigma}_j(\triangle q\cdot(l+1)) + \overline{\sigma}_j(\triangle q\cdot l)\right)}, \tag{29}$$

where $\triangle q = {}^{L}/_{L+1}$ is the step size, L is the amount of discretization points, $j \in \{Hi, Av, Lo\}$ and $\overline{\sigma}_j$ denotes a membership function with removed "top" above the corresponding value of $\mathcal{R}_j$. Thus, the output quantifier is computed via centroid function over $\mathcal{R}_j$ and $q_{\kappa,j}$:

$$q_\kappa = \frac{\sum q_{\kappa,j}\mathcal{R}_j}{\sum \mathcal{R}_j}, j \in \{Hi, Av, Lo\}. \tag{30}$$

Dequantification is, hence, simple: $\kappa_{\text{fuzz}} = \max\{\bar{\kappa}_{\text{fuzz}}, q_\kappa\}$.

E. Stability analysis of the AUKF-FS

In this section, a stability analysis for the AUKF-FS is provided. It is shown that suggested modifications for an UKF do not affect the stochastic boundedness of the estimation error. It is assumed that the measurement model is linear:

$$h_k(x_k) = \mathbf{H}_k x_k,. \tag{31}$$

According to (13) of Section II-B, $\mathbf{H}_k = \mathbf{H} = \begin{pmatrix} \mathbf{O}_{(N+1)\times N} & \mathbf{I}_N & \mathbf{O}_{(N+1)\times(5N+1)} \end{pmatrix}$, where $\mathbf{O}_{l\times m}$ denotes an $l \times m$ zero matrix. Recall firstly the definition of exponential boundedness in mean square [41]:

Definition 3: A stochastic process ϵ_k is said to be exponentially bounded in mean square, if there are real strictly positive numbers α, β and $0 < \vartheta < 1$ such that

$$\mathbb{E}[||\epsilon_k||^2] \leq \alpha||\epsilon_0||^2\vartheta^n + \beta$$

holds for every $k \geq 0$.$||\bullet||$ denotes the Euclidean norm of a vector. The estimation and prediction errors are defined as follows:

$$\begin{aligned} \tilde{x}_k &= x_k - \hat{x}_k, \\ \tilde{x}_{k|k-1} &= x_k - \hat{x}_{k|k-1}. \end{aligned} \tag{32}$$

Suppose functions $f(x_k, u_k, w_{k-1})$ and $h(x_k)$ are of class $\mathbb{C}^\infty$, then according to [42], using Taylor series expansion of the estimate and the true state, the prediction error can be approximated as follows:

$$\tilde{x}_{k|k-1} = \mathbf{F}_k\tilde{x}_{k-1} + q_{k-1}, \tag{33}$$

where the matrix of partial derivatives is: $\mathbf{F}_k = \frac{\partial}{\partial x} f(x, u_k, w_k)\Big|_{x=\hat{x}_{k-1}}$. By analogy, rewrite the innovation covariance as follows:

$$\tilde{y}_k = y_k - \hat{y}_k = \mathbf{H}\tilde{x}_{k|k-1} + r_k. \tag{34}$$

Let the diagonal instrumental matrix be introduced as follows: $\beta_k = \text{diag}\left\{ \beta_{1,k}, \quad \beta_{2,k}, \quad \ldots \quad \beta_{n,k} \right\}$ such that:

$$\tilde{x}_{k|k-1} = \beta_k\mathbf{F}_k\tilde{x}_{k-1} + q_k.$$

Supposing the conditions of Lemma 1 are satisfied and given the adaptation mechanism (25), rewrite the term $\mathbf{A}_k\mathbf{Q}_{k-1}$ of (23) as follows:

$$\mathbf{A}_k\mathbf{Q}_{k-1} = \widetilde{\mathbf{Q}}_k + \triangle\mathbf{Q}_k, \tag{35}$$

where $\widetilde{\mathbf{Q}}_k \leq \tilde{q} < q_{\text{min}}\bar{\kappa}_{\text{fuzz}}$ for some real number $\tilde{q} > 0$. Thus by inspection $\triangle\mathbf{Q}_k \geq q_{\text{min}}\bar{\kappa}_{\text{fuzz}} - \tilde{q} > 0$ since $\mathbf{A}_k\mathbf{Q}_{k-1} \geq q_{\text{min}}\bar{\kappa}_{\text{fuzz}}$ for $k = 0, 1, 2$...Consider an ordinary UKF given in Section II-A with the state noise covariance given as $\widetilde{\mathbf{Q}}_k$. Thus, the AUKF-FS can be interpreted as a modified UKF with the predicted estimate covariance given as follows:

$$\begin{aligned} \hat{\mathbf{P}}_{k|k-1} =& \sum_{i=0}^{2n} \mathcal{W}_c^{(i)} \left(\chi_{k|k-1}^{(i)} - \hat{x}_{k|k-1}\right) \cdot \\ & \left(\chi_{k|k-1}^{(i)} - \hat{x}_{k|k-1}\right)^T + \widetilde{\mathbf{Q}}_k + \triangle\mathbf{Q}_k. \end{aligned} \tag{36}$$

On the other hand, the actual estimate covariance can be expressed as:

$$\begin{aligned} &\bar{\mathbf{P}}_{k|k-1} = \mathbb{E}[\tilde{x}_{k|k-1}\tilde{x}_{k|k-1}^T] = \\ &\mathbb{E}\left[(\beta_k\mathbf{F}_k\tilde{x}_{k-1} + q_k)(\beta_k\mathbf{F}_k\tilde{x}_{k-1} + q_k)^T\right] = \\ &\beta_k\mathbf{F}_k\hat{\mathbf{P}}_{k|k-1}\mathbf{F}_k^T\beta_k + \mathbb{E}\left[(\beta_k\mathbf{F}_k\tilde{x}_{k-1})(\beta_k\mathbf{F}_k\tilde{x}_{k-1})^T\right] - \\ &\beta_k\mathbf{F}_k\hat{\mathbf{P}}_{k|k-1}\mathbf{F}_k^T\beta_k + \widetilde{\mathbf{Q}}_k = \\ &\beta_k\mathbf{F}_k\hat{\mathbf{P}}_{k|k-1}\mathbf{F}_k^T\beta_k + \triangle\mathbf{P}_{k|k-1} + \widetilde{\mathbf{Q}}_k, \end{aligned}$$

with an instrumental matrix $\triangle\mathbf{P}_{k|k-1} = \mathbb{E}\left[(\beta_k\mathbf{F}_k\tilde{x}_{k-1})(\beta_k\mathbf{F}_k\tilde{x}_{k-1})^T\right] - \beta_k\mathbf{F}_k\hat{\mathbf{P}}_{k|k-1}\mathbf{F}_k^T\beta_k$. Consider the residual between the predicted estimate covariance and the actual one: $\delta\mathbf{P}_{k|k-1} = \mathbf{P}_{k|k-1} - \bar{\mathbf{P}}_{k|k-1}$. Thus, (36) can be rewritten as:

$$\hat{\mathbf{P}}_{k|k-1} = \beta_k\mathbf{F}_k\hat{\mathbf{P}}_{k|k-1}\mathbf{F}_k^T\beta_k + \hat{\mathbf{Q}}_k,$$

with $\hat{\mathbf{Q}}_k = \triangle\mathbf{P}_{k|k-1} + \delta\mathbf{P}_{k|k-1} + \widetilde{\mathbf{Q}}_k + \triangle\mathbf{Q}_k$.

Hence, the conditional estimate covariance is:

$$\hat{\mathbf{P}}_k = \hat{\mathbf{P}}_{k|k-1} - \mathbf{K}_k\mathbf{S}_k\mathbf{K}_k^T. \tag{37}$$

Theorem 4: Consider the non-linear system (7) with a linear measurement model (31) and the AUKF-FS given in Section II-A with (22), (25) and reformulated with (35), (36), (37).

Let the following assumptions hold for $k = 0, 1, 2$...:

- the conditions of Lemma 1 are satisfied,
- there are nonzero real numbers $f_{\text{min}}, f_{\text{max}}, h_{\text{min}}, h_{\text{max}}, \beta_{\text{min}}, \beta_{\text{max}}$ such that:
  $f_{\text{min}}^2 \leq \mathbf{F}_k\mathbf{F}_k^T \leq f_{\text{max}}^2$,
  $h_{\text{min}}^2 \leq \mathbf{H}_k\mathbf{H}_k^T \leq h_{\text{max}}^2$,
  $\beta_{\text{min}}^2 \leq \beta_k\beta_k^T \leq \beta_{\text{max}}^2$,
- there are positive real numbers $\hat{q}_{\text{min}}, \hat{q}_{\text{max}}, r_{\text{min}}, \hat{p}_{\text{min}}, \hat{p}_{\text{max}}$ such that:
  $\hat{q}_{\text{min}} \leq \hat{\mathbf{Q}}_k \leq \hat{q}_{\text{max}}$,
  $\mathbf{R}_k \geq r_{\text{min}}\mathbf{I}_m$,
  $\hat{p}_{\text{min}} \leq \hat{\mathbf{P}}_k \leq \hat{p}_{\text{max}}$,

then the estimation error $\tilde{x}_k$ is bounded in mean square.

Proof: Set $\widetilde{\mathbf{Q}}_k \leq \tilde{q} < q_{\text{min}}\bar{\kappa}_{\text{fuzz}}$ according to (35). Further proof of the theorem is given in [42], p. 264, Theorem 1.

Remark 5: It can be seen from the formulation of the AUKF-FS that the term $\mathbf{A}_k\mathbf{Q}_{k-1}$ plays a role of some enlarged state noise covariance $\widetilde{\mathbf{Q}}_k$ in the suggested scheme of a modified UKF from [42], thus, stability is the same as for this set-up. As it was stated by the authors themselves, the term $\triangle\mathbf{Q}_k$ should be adaptively adjusted in response to changing environment, therefore, the AUKF-FS can be considered as one of possible solutions.

III. SIMULATION RESULTS

Simulation was carried out using a multi-body model of the tractor in MATLAB©/SimMechanics™with stochastic input signals, i.e. the draft force and the field micro-profile. Input signals were modeled using statistical characteristics of on-field measurement data. White Gaussian noise was added to the measurement signals in the model to imitate physical sensors. The standard deviation of the measurement noise was set up as follows: 0.1 mps for travelling velocity, 0.1 $^{\mathrm{rad}}/_{\mathrm{s}}$ for wheel speed and 0.25 kN for the draft force and wheel load. The tractor performed tillage on a sandy loam, the working depth was 7.5 cm and width was 5 m. The initial measurement and state covariances are: $\mathbf{R} = \mathrm{diag}\{\ 0.01,\ \ 0.01,\ \ 0.01,\ \ 0.01,\ \ 0.1\ \}$, $\mathbf{Q} = [\ 0.1\cdot\mathbf{I}_4,\ \ 0.01\cdot\mathbf{I}_4,\ \ 10^{-5},\ \ 10^{-5}\cdot\mathbf{I}_{21}\ ]$. Parameters of the FS are the following: $a_{\max} = 3^{\mathrm{m}}/_{\mathrm{s}^2}$, $\bar{\kappa}_{\mathrm{fuzz}} = 0.15$, $L = 10$, $\lambda_{Lo} = 0.05$, $\lambda_{Av} = 0.5$, $\lambda_{Hi} = 0.95$, $\xi = 0.2$ and $\zeta = 2$. Simulation integration step was 1 ms. CAN-bus was modeled with the sample time of 10 ms. Monte-Carlo simulations with 17500 samples were performed for the UKF, AUKF and AUKF-FS. Results of identification of the traction parameters are shown on Fig. 2 and Fig. 3. A measurement failure was simulated at 9 s in the following way: measured v and ω_w were 4 times amplified during 100 ms.

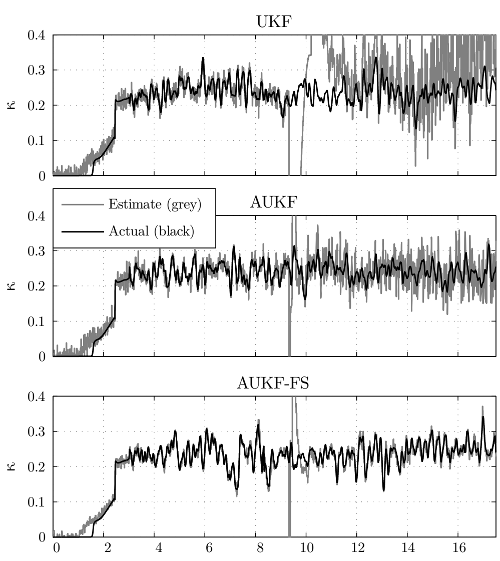

Fig. 2. Identification of the net tractive ratio

The results show that the ordinary UKF does not provide convergent estimate after the measurement failure happens.

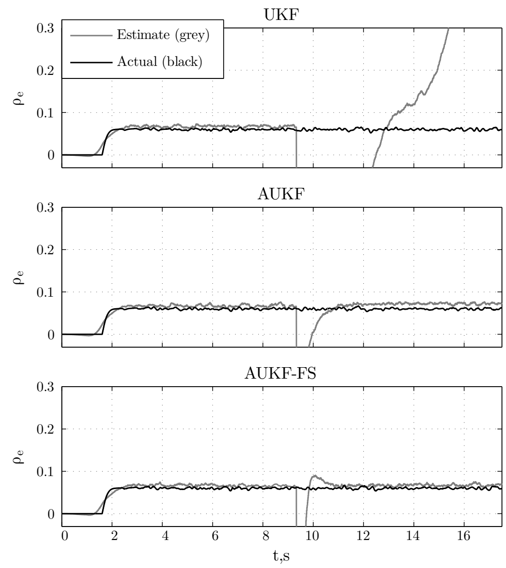

Fig. 3. Identification of the external rolling resistance coefficient

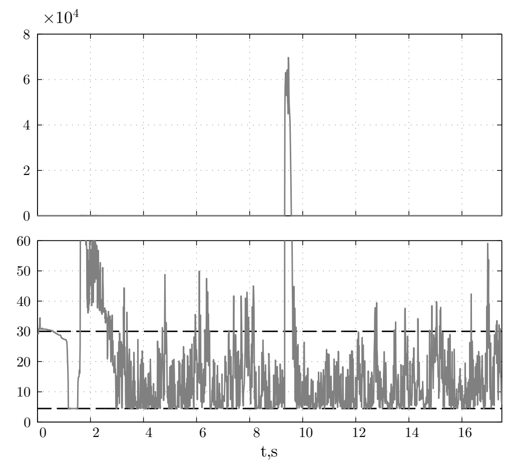

Fig. 4. Trace of the adaptive matrix $\mathbf{A}_k$. Measurement failure is at 9 s. Bottom dashed line shows $n\bar{\kappa}_{\mathrm{fuzz}}$ and the top line is n

The AUKF is able to restore convergence, but the elements of the state noise covariance $\mathbf{Q}$ become high. This affects estimation of the friction force coefficients μ and due to high dispersion of them, ρ_e becomes slightly biased. The estimate of κ is highly noisy. The AUKF-FS overcomes the measurement failure as well, but restores its $\mathbf{Q}$ back to normal mode according to the algorithm (25). Notice that the AUKF-FS also provides smoother estimate in the normal mode before the measurement failure happens. The normalized root mean squared error (NRMSE) of the net tractive ratio κ estimates in time range 10...17.5 s was 57.3, 11.9 and 3.81 % for the UKF, AUKF and AUKF-FS respectively. For the external rolling resistance coefficient ρ_e, these values were $>$100, 20.96 and 1.02 % for the UKF, AUKF and AUKF-FS respectively. By analyzing (4), it is seen that during the measurement fault the adaptation mechanism of the AUKF-FS increases the $\mathbf{A}_k$ and thus $\mathbf{Q}_k$ to restore convergence. This process is consistent with the FS, i.e. the FS sets only the lower bound when the filter works normally.

IV. Experimental results

Laboratory tests for verification of the identification system based on the AUKF-FS were carried out at the AST. Experimental set-up consists of the specially installed prototype tractor RigiTrac EWD 120 equipped with electrical single-wheel drives. The general view of the laboratory stand is given on Fig. 5.

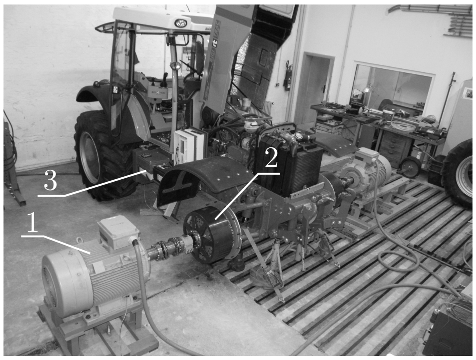

Fig. 5. Laboratory stand. On the picture: 1 - electrical load machine, 2 - electrical motor, 3 - power electronics

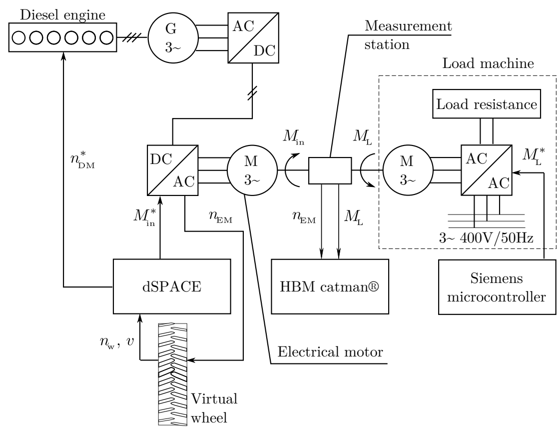

Fig. 6. Experimental set-up

Fig. 6 illustrates the experimental set-up. At the current stage, the experiments were carried out together with a TCS in couple with an imitation of a wheel (so-called "virtual wheel"). The electriacl load machine imitated on-field conditions in a from of a load torque. The travelling velocity of the virtual wheel was imitated. From this signal and from the electrical motor speed, virtual wheel slip was determined. The TCS held it at the desired value by compensatinf the load torque. The AUKF-FS and TCS were implemented into dSPACE MicroAutoBox from a computer by means of DS1103 PC-card. Additionally, DS 815 card was used to load the program code. Connection of virtual channels, which are programmed in the MATLAB©/SimMechanics™model, to physical CAN-bus channels was performed using dSPACE-Toolbox. At this stage, sampling times, addresses and data frame structure for CAN-bus channels were configured. Execution of the program algorithm was performed by means of RealTime-Toolbox. In the experiment, the command of the input torque M^*_{in} was generated. The desired value of the load torque M^*_L was set up by a microcontroller from Siemens. The desired diesel engine speed n^*_{DM} was set up manually. The contactless measurement station from HBM has functions to measure both the speed n_{EM} and torque M_L. Measurement accuracy is of class less than 0.5 %. The experiments were carried out in several stages with different ranges of the load toque and with controller modes. The estimated load torque was compared with that from the load machine. Results of one of the experiments are given on Fig. 7 as an example. It can be seen that the dynamics of the electrical motor together with the load machine has a specific oscillatory component with frequency of about 5.5 Hz which was likely due to mechanical properties of the construction. In the test stand, such effects are not significant, but nevertheless, the identification system was able to track this dynamics with appropriate accuracy. This ability becomes important in the field operation where dynamical components arise from multiple different sources and have significant impact on traction. In all experiments, NRMSE of estimation was below 5 %.

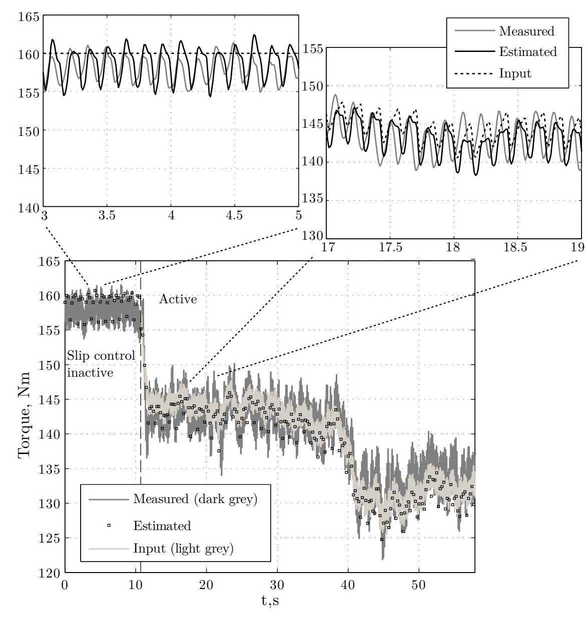

Fig. 7. Estimation of the load machine torque in phases of active/inactive slip control. For the sake of clarity, the estimate in the bottom part is sampled every 0.25 s

V. Conclusions

In the present paper, a new algorithm of adaptive filtering for the UKF in application to tractor dynamics was designed. The basic idea of this approach comprises a combination of somewhat conventional adaptation algorithm applied for the state noise covariance and a fuzzy logic system, namely a fuzzy supervisor. The main goal of it is to additionally adjust the state noise covariance in order to achieve smoother estimate while keeping the abilities of the adaptation algorithm to eliminate divergence in case of measurement or estimation failures. It was shown that incorporation of the FS into the AUKF does not affect stability of the estimation error in mean square. Simulations results have shown the ability of the AUKF-FS to eliminate divergence as well as the AUKF and estimate the traction parameters with better quality in the stable mode. The new filter was successfully experimentally tested using the tractor with electrical single-wheel drives.

REFERENCES

[1] B. Bernhard, "Hybrid drives for off-road vehicles," in *FISITA World Automotive Congress, Barcelona, Spain*, 2004, pp. 23–27.

[2] M. Wünsche, *Electrical single wheel drives for tractors (in German)*. TUDpress, 2005.

[3] M. Geissler, W. Aumer, M. Lindner, and T. Herlitzius, "Electric single wheel drive for mobile agricultural machinery," *Landtechnik*, vol. 5, pp. 368–371, 2010.

[4] K. T. Renius *et al.*, *Tractors. Technology and its application.* BLV Verlagsgesellschaft, 1985.

[5] U. Kiencke and L. Nielsen, *Automotive Control Systems*. Springer-Verlag, 2005.

[6] B. Pichlmaier, "Traction management for tractors (in German)," Ph.D. dissertation, München, Technische Universität München, Diss., 2012, 2012.

[7] H. Pacejka, *Tyre and vehicle dynamics*. Butterworth-Heinemann, 2005.

[8] J. Y. Wong, *Theory of ground vehicles*. Wiley, 2008.

[9] T. Nakakuki, T. Shen, and K. Tamura, "Adaptive control approach to uncertain longitudinal tire slip in traction control of vehicles," *Asian Journal of Control*, vol. 10, no. 1, pp. 67–73, Jan 2008.

[10] E. Ono, K. Asano, M. Sugai, S. Ito, M. Yamamoto, M. Sawada, and Y. Yasui, "Estimation of automotive tire force characteristics using wheel velocity," *Control Eng. Practice*, vol. 11, pp. 1361–1370, 2003.

[11] J. Villagra, B. dAndra Novel, M. Fliess, and H. Mounier, "A diagnosis-based approach for tire-road forces and maximum friction estimation," *Control Engineering Practice*, vol. 19, no. 2, pp. 174–184, Feb 2011.

[12] J. Matuško, I. Petrović, and N. Perić, "Neural network based tire/road friction force estimation," *Engineering Applications of Artificial Intelligence*, vol. 21, no. 3, pp. 442–456, Apr 2008.

[13] C. Canudas-de Wit, M. L. Petersen, and A. Shiriaev, "A new nonlinear observer for tire/road distributed contact friction," in *Decision and Control, 2003. Proceedings. 42nd IEEE Conference on*, vol. 3. IEEE, 2003, pp. 2246–2251.

[14] L. R. Ray, "Nonlinear tire force estimation and road friction identification: Simulation and experiments," *Automatica*, vol. 33, no. 10, pp. 1819–1833, 1997.

[15] J. Dakhlallah, S. Glaser, S. Mammar, and Y. Sebsadji, "Tire-road forces estimation using extended kalman filter and sideslip angle evaluation."IEEE, Jun 2008, pp. 4597–4602.

[16] X. Zhu, C. Qiu, L. Guo, and Y. Zhang, "New method for slip and tire force estimation of wheeled mobile robot on inclined terrain," in *Robotics and Biomimetics (ROBIO), 2011 IEEE International Conference on*. IEEE, 2011, pp. 2264–2269.

[17] R. Van Der Merwe, E. A. Wan, and S. Julier, "Sigma-point kalman filters for nonlinear estimation and sensor-fusion-applications to integrated navigation," in *Proceedings of the AIAA Guidance, Navigation & Control Conference*, 2004, pp. 16–19.

[18] E. Wan and R. Van Der Merwe, "The unscented kalman filter for nonlinear estimation." IEEE, 2000, pp. 153–158.

[19] Z. Zhang and J. Zhang, "A novel strong tracking finite-difference extended kalman filter for nonlinear eye tracking," *Sci China Ser F-Inf Sci*, vol. 52, no. 4, pp. 688–694, Apr 2009.

[20] R. Fitzgerald, "Divergence of the Kalman filter," vol. 16, no. 6, pp. 736–747, 1971.

[21] A. H. Mohamed and K. P. Schwarz, "Adaptive kalman filtering for ins/gps," *J. Geodesy*, vol. 73, no. 4, pp. 193–203, 1999.

[22] E. P. Herrera, R. Quirós, and H. Kaufmann, "Analysis of a kalman approach for a pedestrian positioning system in indoor environments," in *Euro-Par 2007 Parallel Processing*. Springer, 2007, pp. 931–940.

[23] H. E. Soken and C. Hajiyev, "Adaptive unscented Kalman filter with multiple fading factors for pico satellite attitude estimation," in *Proc. 4th Int. Conf. Recent Advances in Space Technologies RAST '09*, 2009, pp. 541–546.

[24] P. Cui and H. Zhang, "Qmrpf-ukf master-slave filtering for the attitude determination of micro-nano satellites using gyro and magnetometer," *Sensors*, vol. 10, no. 11, pp. 9935–9947, Nov 2010.

[25] Q. Song and J.-D. Han, "An adaptive ukf algorithm for the state and parameter estimations of a mobile robot," *Acta Automatica Sinica*, vol. 34, no. 1, pp. 72–79, May 2008.

[26] Q. Song and Y. He, "Adaptive unscented kalman filter for estimation of modelling errors for helicopter," in *Robotics and Biomimetics (ROBIO), 2009 IEEE International Conference on*. IEEE, 2009, pp. 2463–2467.

[27] L. Zhao and X. Wang, "An adaptive ukf with noise statistic estimator." IEEE, May 2009, pp. 614–618.

[28] S. Zhang, "An adaptive unscented Kalman filter for dead reckoning systems," in *Proc. Int. Conf. Information Engineering and Computer Science ICIECS 2009*, 2009, pp. 1–4.

[29] G. Hu, S. Gao, and L. Xue, "A novel adaptive unscented Kalman filter," in *Proc. Third Int Intelligent Control and Information Processing (ICICIP) Conf*, 2012, pp. 497–502.

[30] V. Fathabadi, M. Shahbazian, K. Salahshour, and L. Jargani, "Comparison of adaptive kalman filter methods in state estimation of a nonlinear system using asynchronous measurements," in *Proc., World Congress on Engineering and Computer Science*, vol. 2, 2009, pp. 1–8.

[31] G. Abdelnour, S. Chand, and S. Chiu, "Applying fuzzy logic to the Kalman filter divergence problem," in *Proc. Conf. Int Systems, Man and Cybernetics 'Systems Engineering in the Service of Humans'*, 1993, pp. 630–635.

[32] P. Escamilla-Ambrosio and N. Mort, "Adaptive kalman filtering through fuzzy logic," in *Proc. of the 7th UK Workshop on Fuzzy System, Recent Advances and Practical Applications of Fuzzy, Nero-Fuzzy, and Genetic Algorithm-Based Fuzzy Systems, UK, Sheffield*, 2000, pp. 67–73.

[33] R. Havangi, M. A. Nekoui, and M. Teshnehlab, "Adaptive neuro-fuzzy extended kaiman filtering for robot localization," in *Power Electronics and Motion Control Conference (EPE/PEMC), 2010 14th International*. IEEE, 2010, pp. T5–130.

[34] D.-J. Jwo and S.-Y. Lai, "Navigation integration using the fuzzy strong tracking unscented kalman filter," *Journal of Navigation*, vol. 62, no. 02, p. 303, Apr 2009.

[35] X. Tian, Y. P. Cao, and S. Chen, "Process fault prognosis using a fuzzy-adaptive unscented kalman predictor," *International Journal of Adaptive Control and Signal Processing*, vol. 25, no. 9, pp. 813–830, Sep 2011.

[36] S. J. Julier, Jeffrey, and K. Uhlmann, "Unscented filtering and nonlinear estimation," 2004.

[37] V. Guskov, N. Velev, Y. Atamanov, N. Bocharov, I. Ksenevich, and A. Solonsky, "Tractors. theory (in Russian)," *Mashinostroenie*, 1988.

[38] M. Doumiati, A. Victorino, A. Charara, D. Lechner, and G. Baffet, "An estimation process for vehicle wheel-ground contact normal forces," *IFAC WC*, pp. 7110–7115 , vol. 8, 2008.

[39] M. Schreiber and H. Kutzbach, "Comparison of different zero-slip definitions and a proposal to standardize tire traction performance," *Journal of Terramechanics*, vol. 44, no. 1, pp. 75–79, Jan 2007.

[40] A. Almagbile, J. Wang, and W. Ding, "Evaluating the performances of adaptive kalman filter methods in gps/ins integration," *Journal of Global Positioning Systems*, vol. 9, no. 1, pp. 33–40, Jun 2010.

[41] K. Reif, S. Gunther, E. Yaz, and R. Unbehauen, "Stochastic stability of the discrete-time extended kalman filter," *IEEE Transactions on Automatic Control*, vol. 44, no. 4, pp. 714–728, Apr 1999.

[42] K. Xiong, H. Zhang, and C. Chan, "Performance evaluation of ukf-based nonlinear filtering," *Automatica*, vol. 42, no. 2, pp. 261–270, Feb 2006.